

Reconstructing Aircraft Turn Manoeuvres for Trajectory Analyses Using ADS-B Data

Junzi Sun, Joost Ellerbroek, and Jacco M. Hoekstra

Faculty of Aerospace Engineering
Delft University of Technology
Delft, the Netherlands
j.sun-1, j.ellerbroek, j.m.hoekstra@tudelft.nl

Abstract—The Automatic Dependent Surveillance-Broadcast (ADS-B) data has become one of the most popular sources of data for trajectory-based ATM studies. It can be received in most of the world without restrictions. Extended coverage can be achieved with a network of low-cost receivers and satellites. However, the fact that ADS-B is designed to contain only a low number of aircraft states such as position and velocity poses a challenge for some trajectory-based studies, for example, using ADS-B data to study aircraft turns. To this extent, air traffic controllers commonly rely on Mode-S track and turn reports to gather additional information like bank angle and turn rates during turns. Unlike ADS-B, this data has a low update rate and is not always openly available for all researchers. In this paper, we propose methods that allow researchers to extract and analyze aircraft turn parameters from ADS-B data during offline flight analysis. The paper first discusses the dynamics of aircraft turns. Then, based on ADS-B trajectory data, several steps are designed to derive turn radius, bank angle, and turn rate of an aircraft. The estimation results are validated with aircraft track and turn reports from Mode S Enhanced Surveillance. The median errors for bank angle and turn rate are found to be less than 2 degrees and 0.1 degrees/s respectively, which reflects the accuracy of the estimation approach.

Keywords - aircraft performance, turn performance, bank angle, load factor, ADS-B, data analysis

NOMENCLATURE

| | | |
|--------------|----------------------------|-------------------|
| χ | track angle | deg |
| \mathbf{A} | transformation matrix | - |
| lat | latitude | deg |
| lon | longitude | deg |
| ω | turn rate | deg |
| ϕ | bank angle | deg |
| ψ | heading angle | deg |
| ρ | air density | kg/m ³ |
| C_L | lift coefficient | - |
| F_c | centrifugal force | N |
| g | gravitational acceleration | m/s ² |
| h | altitude | m |
| L | total lift | N |
| m | aircraft mass | kg |
| R_t | radius of the turn | m |
| V | velocity, true air speed | m/s |
| W | aircraft weight | N |

I. INTRODUCTION

With the increased utilization of Mode-S extended squitter on commercial aircraft, air traffic management research has entered a new era. The vast amount of ADS-B data gathered by large-scale receiver networks, such as FlightRadar24 and the OpenSky-network [1], has enabled many new data-based trajectory studies. Several open-source tools [2], [3] have been developed in recent years that allow researchers to better harvest information from this new data source.

ADS-B is a valuable data source for macroscopic level studies due to its high accuracy, availability, and extended coverage. However, it falls short for microscopic studies, especially in situations where low-level aircraft dynamics are required. This is due to the lack of aircraft parameter varieties provided by ADS-B, which is primarily dominated by position and speed. Other information including identification and operations status are broadcast at much lower update rates. The rotations (pitch, roll, and yaw angles) are never transmitted through ADS-B. However, better knowledge of some of these parameters, such as roll angle (or bank angle), would allow better calculation of aircraft lift and drag, which, in turn, can improve the accuracy of mass and fuel consumption estimations studies [4]. A recent study on bank angle was conducted based on 2D radar data to study the track and guidance in turn [5].

This paper focuses on answering the research question of how to better estimate low-level performance parameters during turns based on a previous preliminary study [6]. There are several challenges while trying to address this question. For instance, the low temporal resolution of turns leads to a small number of data points, and the simplified point-mass performance model used in most air transportation studies sometimes ignores the rotations of aircraft. Addressing these challenges, the primary goal of this paper is to estimate performance parameters for individual turns using only ADS-B data. These parameters include turn radius, roll angle, load factor, and turn rate. Additional track and turn reports from Mode S Enhanced Surveillance (EHS) are used to construct the validation dataset.

The remainder of the paper is designed as follows. In section two, we first address the fundamental principles of aircraft

turns. In section three, the method used to extract turns from ADS-B flight trajectories is derived. In section four, processes and steps for estimating different turn performance parameters are given. Then, in section five, we show the results of our method based on a large number of flights from different aircraft types. Finally, in sections six and seven, discussions and conclusions are provided.

II. COORDINATED TURNS

A turning flight is defined as a continuous change of path direction. Commonly, coordinated turns are performed to maintain passenger comfort and the safety of flights. The manoeuvre requires the coordination of different control surfaces and thrust. When an aircraft turns, the ailerons are deflected to provide the desired roll angle. The rudder of the aircraft also needs to be deflected to provide the corresponding yaw angle of the aircraft. The roll manoeuvre changes the direction of lift and leads to a decrease in the vertical lift component. Thus, the aircraft needs to increase its pitch angle (by deflecting the elevator) to increase the total lift. The increased lift causes an increase in total drag. Hence, the thrust also needs to be adjusted correspondingly to maintain the same speed.

During a coordinated turn, the aircraft flies at a certain bank angle ϕ and turn rate ω , depending on the velocity and combination of forces (lift L , weight W , and centrifugal force F_c). The kinematic and kinetic components are illustrated in Figure 1.

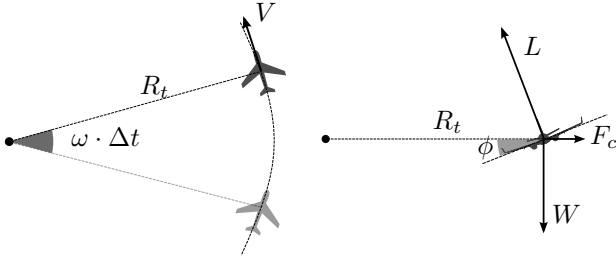


Figure 1. Aircraft coordinated turn

For a coordinated turn where the airspeed and altitude are constant, the relationship of different performance parameters can be described as follows [7]:

$$F_c = L \sin \phi = \frac{W V^2}{g R_t} \quad (1)$$

$$W = L \cos \phi \cos \gamma \quad (2)$$

where V is the airspeed, R_t is the radius of the turn, and γ is the flight path angle. The load factor (denoted as n) is defined as the ratio of lift to the aircraft weight:

$$n = \frac{L}{W} \quad (3)$$

It can be calculated separately from Equations 1 and 2 as:

$$n = \frac{V^2}{g R_t \sin \phi} \quad (4)$$

$$n = \frac{1}{\cos \phi \cos \gamma} \quad (5)$$

By combining these two equations, the bank angle can be calculated from the aircraft turn radius, airspeed, and flight path angle (during climb or descent) as follows:

$$\phi = \arctan \left(\frac{V^2 \cos \gamma}{g R_t} \right) \quad (6)$$

Equations 4 and 6 are the basis for estimate load factor and bank angle during the turn. However, one of the hidden parameters, the turn radius (R_t) needs to be first derived based on the ADS-B turn trajectory.

III. TURN TRAJECTORY EXTRACTION

The first challenge we are facing is to extract the turning segments of the flight from the ADS-B trajectory data. To identify the turns, aircraft headings are used as an indicator. An example of a heading profile from one trajectory is illustrated in Figure 2. In this example, we can see several heading changes occurring during a period of 500 seconds.

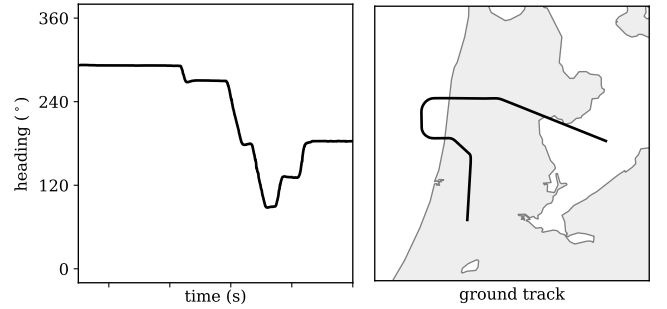


Figure 2. An example trajectory with turns (headings and ground track)

Aircraft track angle (χ) can be calculated from the ADS-B velocity reports using the south-north and west-east components of the ground velocity. Assuming zero (or calm) wind, the track angle is approximately the same as the heading (ψ):

$$\psi \approx \chi \quad (7)$$

The value of heading (or track) angle ranges from 0° to 360° to the direction of true north. To consider the continuity of the heading (jumps between 0° and 360°), a new function is designed to calculate the changes in track angle as:

$$n_x(t) = \sin \psi(t) \quad (8)$$

$$n_y(t) = \cos \psi(t) \quad (9)$$

$$\Delta'_n(t) = \frac{d\psi}{|d\psi|} \frac{\sqrt{dn_x^2 + dn_y^2}}{dt} \quad (10)$$

where Δ'_n represents the change in the difference between two norm vectors, which have the same angles as two consecutive heading measurements. We then keep and scale Δ'_n values that are larger than a threshold.

$$\Delta'_{n,s}(t) = \begin{cases} 20 + \Delta'_n(t) & \Delta'_n(t) > \sin(1^\circ) \\ -20 + \Delta'_n(t) & \Delta'_n(t) < -\sin(1^\circ) \end{cases} \quad (11)$$

This identification process is illustrated in Figures 3 and 4. Figure 3 shows the profile of Δ'_n in the flight data. It also presents the potential time windows in which turns occur by comparing new parameter $\Delta'_{n,s}$ with Δ'_n .

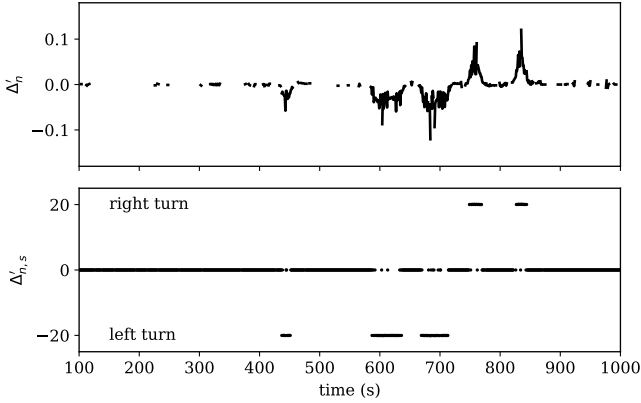


Figure 3. Extraction of turns from trajectory data

Based on the new $\Delta'_{n,s}$, the turning time window can be identified based on clustering algorithms (for example, DBSCAN [8]). The clustering algorithm can conveniently filter out the outliers (points with $\Delta'_{n,s} = 0$) within each potential time window and identify the start and end of each turn. Finally, Figure 4 visualizes the turn segments in a the example trajectory.

IV. TURN PERFORMANCE ESTIMATION

Once the turns from the trajectories are extracted, performance parameters such as turning radius, bank angle, and load factor can be estimated individually.

The first step is to calculate the turning radius from the trajectory data. Trajectories consist of latitudes, longitudes, and altitudes. To simplify the calculation, we first convert the trajectories to three-dimensional Cartesian coordinates with the references to the center of the Earth using the spherical Earth model:

$$\begin{aligned} x &= (R_e + h) \cos(\text{lat}) \cos(\text{lon}) \\ y &= (R_e + h) \cos(\text{lat}) \sin(\text{lon}) \\ z &= (R_e + h) \sin(\text{lat}) \end{aligned} \quad (12)$$

where the R_e , h , lat , and lon are the radius of the Earth, altitudes, latitudes, and longitudes of the aircraft respectively.

Based on these coordinates, one can find a circle that best describes the trajectory using the least-squares regression. The

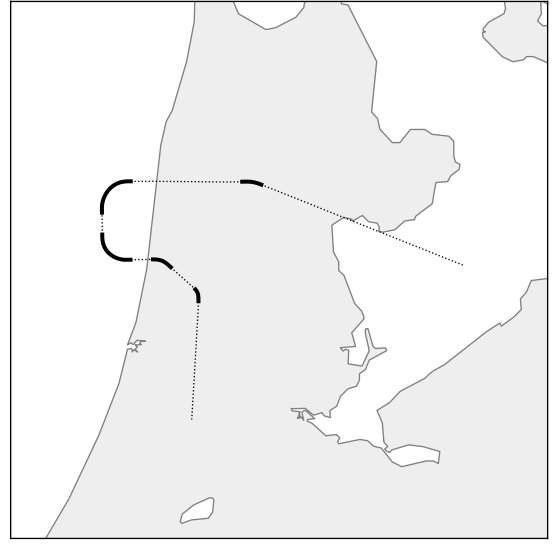


Figure 4. Trajectory ground track with turns identified

radius of this circle should correspond to the aircraft turn radius. However, the variance of the least-squares fit of a circle to the three-dimensional points can be large. This sometimes prevents the best circle from being found. We first need to reduce the least-squares problem from three dimensions to two dimensions to help decrease the uncertainties in the regression method.

To reduce the dimension of the positions, a two-dimensional plane in the three-dimensional space first needs to be found, where the squared-sum of the distances from all points is minimized (i.e., the plane that aligns best with the set of positions or the turn). After that, we can use the projection of the points on the plane to find the ideal circle.

We define the plane using any point \vec{p}_0 within the plane and a normal vector \vec{n} to the plane (see Figure 5):

$$\vec{p}_0 = [x_0, y_0, z_0]^T \quad (13)$$

$$\vec{n} = [1, \alpha_p, \alpha_a]^T \quad (14)$$

$$= [\sin \alpha_p \cos \alpha_a, \sin \alpha_p \sin \alpha_a, \cos \alpha_p]^T \quad (15)$$

where α_p is the polar angle and α_a is the azimuth angle. The first equation of \vec{n} is the spherical representation, while the second equation is the Cartesian representation. For all positions \mathbf{p} , the distances to the plane can be computed as the dot product of the distance between each position to \vec{p}_0 and the normal vector:

$$\mathbf{d} = \vec{n} \cdot (\mathbf{p} - \vec{p}_0) \quad (16)$$

The best plane can be found when the squared-sum of all distances to the plane is minimized:

$$\vec{p}_0, \vec{n} = \underset{\vec{p}_0, \vec{n}}{\operatorname{argmin}} \sum_{i=1}^n d_i^2 \quad (17)$$

Next, we transform the fitted plane to the reference x,y-plane. This step will transform the radius calculation from a 3D problem to a 2D problem. To do so, a transformation matrix needs to be found. The transformation matrix can be calculated using three points from the previously found plane (p_0 , u_0 , and v_0) and the x,y-plane (p_1 , u_1 , and v_1), which satisfies the following relation:

$$\vec{u}_0 = \frac{\vec{m} \times \vec{n}}{\|\vec{m} \times \vec{n}\|} \quad (18)$$

$$\vec{v}_0 = \vec{u}_0 \times \vec{n} \quad (19)$$

$$\vec{p}_1 = [0, 0, 0]^T \quad (20)$$

$$\vec{u}_1 = [1, 0, 0]^T \quad (21)$$

$$\vec{v}_1 = [0, 1, 0]^T \quad (22)$$

$$(23)$$

where \vec{m} can be any vector that is not parallel to \vec{n} . Then, the transformation (A) can be computed as:

$$\mathbf{A} = [\vec{p}_1, \vec{u}_1, \vec{v}_1] [\vec{p}_0, \vec{p}_0 + \vec{u}_0, \vec{p}_0 + \vec{v}_0]^{-1} \quad (24)$$

To convert all positions p to x,y-plane points p_{xy} , the following equations are applied:

$$p_{xy} = \mathbf{A}p \quad (25)$$

In Figure 5, such a transformation is illustrated. The original coordinates are shown on the left-hand side, while the new projection is shown on the right-hand side of the illustration.

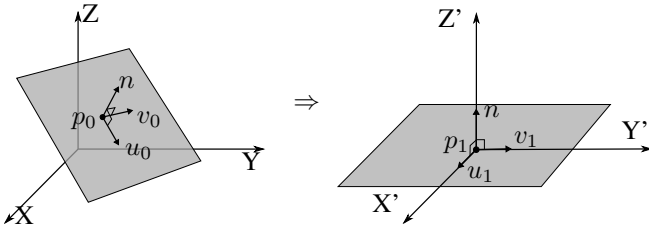


Figure 5. The rotation of the trajectory plane from 3D to 2D

It is worth noting that after the transformation, the points p_{xy} maintain the same geometrical distances as the original three-dimensional positions, except the small distances from the original points to the fitted two-dimensional plane are ignored. As an illustration, one of the trajectory transformations is shown in Figure 6.

Once positions are projected to the reference x,y-plane, it becomes simpler to calculate the turn radius. There are several ways to fit a circle to 2D data points [9], [10]. In this paper, we achieve the circle fitting by using the least-squares regression to find the best arc that describes the projected trajectory. First, define the circle as:

$$(x - x_0)^2 + (y - y_0)^2 = R_t^2 \quad (26)$$

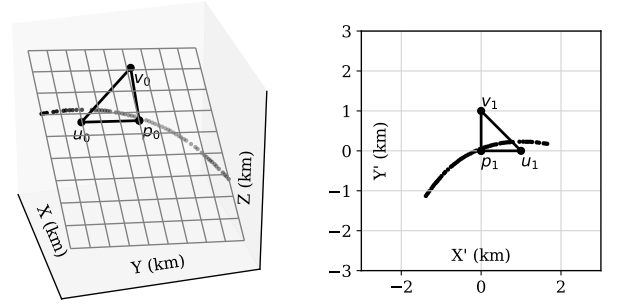


Figure 6. Transformation of 3D positions to 2D positions

For all positions (x_i, y_i) in p_{xy} , the center of the turn (x_0, y_0) and the turn radius R_t can be found when the following condition is satisfied:

$$x_0, y_0, R_t = \operatorname{argmin}_{x_0, y_0, R_t} \sum_{i=1}^n [(x_i - x_0)^2 + (y_i - y_0)^2 - R_t^2]^2 \quad (27)$$

When turning radius and aircraft speed are known, bank angle (ϕ), load factor (n), and turn rate (ω) can be computed conveniently:

$$\phi = \arctan \left(\frac{V^2 \cos \gamma}{g R_t} \right) \quad (28)$$

$$n = \frac{1}{\cos \phi \cos \gamma} \quad (29)$$

$$\omega = \frac{d\psi}{dt} = \frac{V}{R_t} \quad (30)$$

Considering the possible fluctuations in ADS-B velocity reports, the mean speed is used for V in previous equations. Based on these calculations, the example trajectory from Figure 3 yields a turn radius and turn rate, as shown in Figure 7.

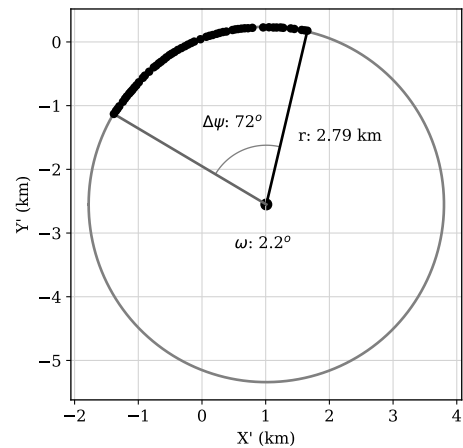


Figure 7. Computation of turn radius and turn rate for an example trajectory

V. EXPERIMENTS AND RESULTS

A. Experiment and validation data

Secondary surveillance radar in Europe selectively interrogates aircraft with a set of reports defined in the Mode-S Enhanced Surveillance protocol. Among others, the *track and turn reports* are down-linked by aircraft. In our earlier research, we developed the method to identify and decode these messages [11]. With the open-source pyModeS tool, these messages can be easily decoded. The track and turn reports have a much lower update rate than ADS-B messages and are not always available. However, it is a good alternative data source to validate the results of the method proposed in this paper.

We make use of a one-month long Mode-S dataset to evaluate the method. In this dataset, both ADS-B and Comm-B messages are recorded by a receiver set up at the Aerospace Engineering faculty of the TU Delft in April 2018.

The turning trajectories of aircraft are extracted from the dataset. When Mode-S track and turn reports are available, we decode and save the roll and track rate information related to the respective turn. This allows us to have validation data alongside the trajectories that are to be used for performance analysis.

In total, 17 common aircraft types are considered in the experiment, where around 800 turns are extracted for each aircraft type. Because some aircraft types are more common than others, the final number of turns per aircraft type differs. For example, the data shows a higher number of Airbus A320 and Boeing 737 aircraft, and a lower number of Airbus A380 or Boeing 787 aircraft. The number of extracted turns per aircraft type is summarized in Table I.

TABLE I
STATISTICS OF THE TURN TRAJECTORY DATASET

| Aircraft | Number of turns | Number of validations | |
|----------|-----------------|-----------------------|-----------|
| | | Bank angle | Turn rate |
| A319 | 992 | 814 | 814 |
| A320 | 999 | 805 | 805 |
| A321 | 994 | 830 | 829 |
| A332 | 998 | 798 | 799 |
| A333 | 998 | 853 | 851 |
| A343 | 82 | 70 | 70 |
| A388 | 159 | 107 | 106 |
| B737 | 998 | 753 | 753 |
| B738 | 996 | 820 | 819 |
| B739 | 1001 | 823 | 823 |
| B744 | 1000 | 850 | 849 |
| B752 | 721 | 596 | 596 |
| B763 | 990 | 842 | 842 |
| B77W | 999 | 789 | 13 |
| B788 | 577 | 465 | 465 |
| B789 | 999 | 837 | 837 |
| E190 | 974 | 728 | 728 |

B. Results

For each turn trajectory extracted from the ADS-B flight data, we are able to estimate the bank angle, turn rate, and

the load factor. The results are shown in Figures 8, 10, and 11 respectively.

In Figure 8, the common bank angle is shown to be around 20 degrees. During actual flight operations, the majority of bank angles range from approximately 12 degrees to 22 degrees.

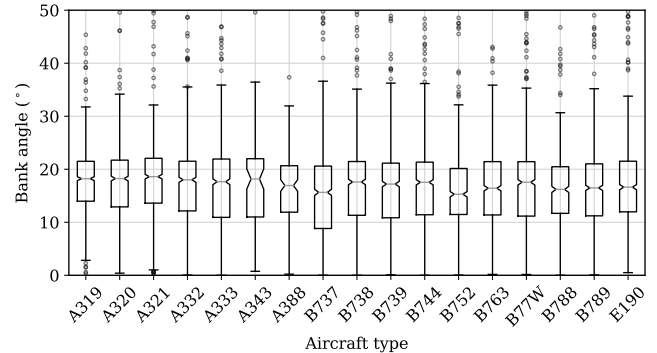


Figure 8. Distribution of estimated bank angles per aircraft type (outliers larger than 50 degrees are not shown)

In Figure 9, the corresponding flight path angles during the turns are shown. The majority of the flight path angles during the turns are below 6 degrees for all aircraft types.

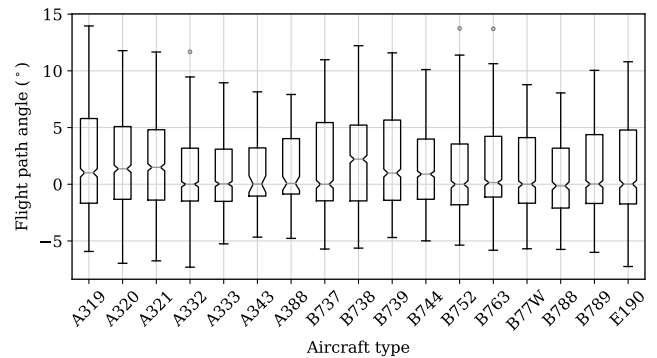


Figure 9. Distribution of flight path angles during the turns per aircraft type

In Figure 10, the common turn rates are shown to be around 1.5 degree/s. This result corresponds well to the standard *rate half* turn, which completes a 360° turn in four minutes.

In Figure 11, the common corresponding load factor for airliners is found to be around 1.05. For airliners, turning with a low load factor is also a key aspect to ensure the comfort of passengers.

C. Accuracy

Comparing the estimated bank angle and turn rate with the values obtained for Mode-S BDS 50 messages, it is also possible to examine the estimation error. The error is calculated as the difference between the median bank angle obtained from the track and turn report and our estimation. The statistics of estimation errors are shown in Figures 12 and 13 for bank angle and turn rate respectively.

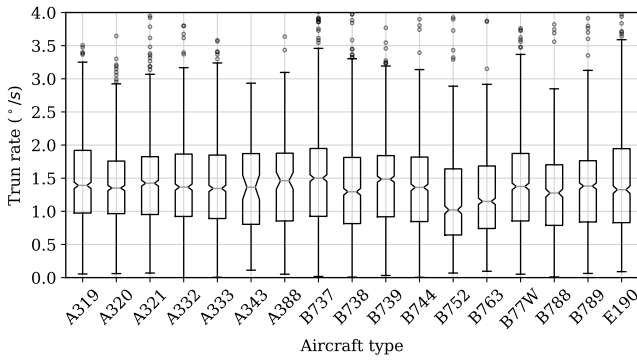


Figure 10. Distribution of estimated turn rate per aircraft type (outliers larger than 4.0 deg/s are not shown)

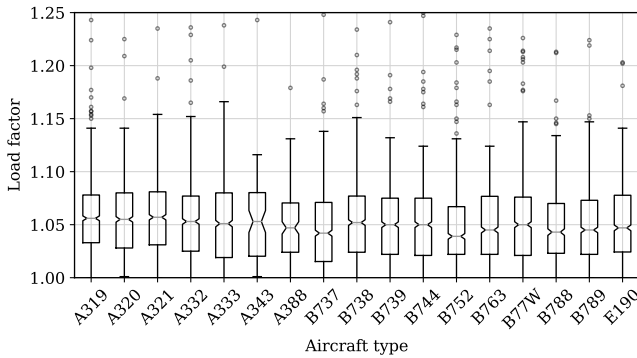


Figure 11. Distribution of estimated load factor per aircraft type (outliers larger than 1.25 are not shown)

Based on these statistics, the median of bank angle error is calculated as less than 2 degrees among all available aircraft types. The median of turn rate error is less than 0.1 degrees/s among all available aircraft types. The overall positive median difference indicates a small but not significant under-estimation with the proposed method.

D. Correlation between speed and bank angle

Using the previous experiment data, we can study the correlation between the bank angle and speed. In Figure 14, the Pearson correlation coefficients are computed for each aircraft type. Based on the results of this figure, weak correlations are found for most of the aircraft types.

Aircraft maximum bank angle and speed are designed to ensure a level of safety. In theory, a strong correlation exists between these two parameters. However, based on the weak correlation between the actual bank angle and speed indicated in Figure 14, we can infer that for most turns, large margins exist between the maximum allowed bank angle and the actual bank angle.

VI. DISCUSSION

A. Mode-S track and turn report

In this study, one of the data sources for measuring turn performance is the track and turn report from the Mode-S

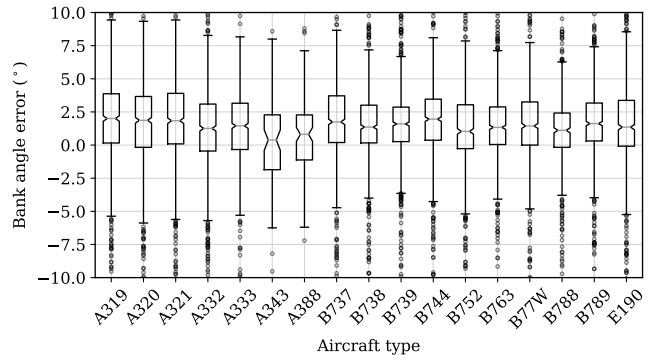


Figure 12. Distribution of bank angle estimation error per aircraft type

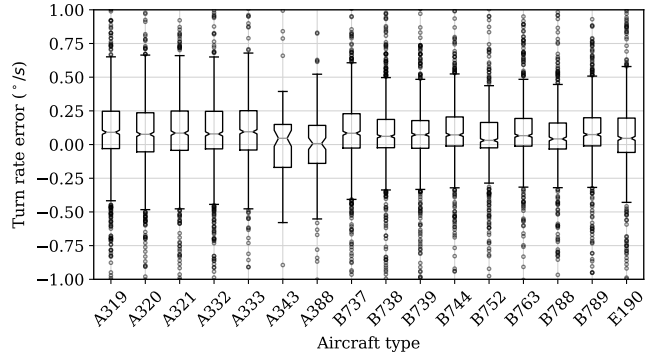


Figure 13. Distribution of turn rate estimation error per aircraft type

secondary surveillance communications. The roll angle and track rate from the track and turn report are used to validate the estimated values of bank angle and turn rate.

Although it offers a direct method to obtain turn performance, the track and turn report has a much lower level of availability. These reports are selectively interrogated at a lower frequency than the ADS-B broadcast rate. For some trajectories, no track and turn report has been intercepted during the turns. The difference in the number of turns and the number of validations, as shown in Table I, reflects this fact. Even when this information is interrogated, not all parameters are available in some cases. For example, most of the track rates are not included in Boeing 777-300ER (B77W) track and turn reports.

Other than the lower availability compared to ADS-B messages, the data in the track and turn reports are prone to large variations based on observations. To this extent, the median values of bank angle and turn rates are used in the validation. However, based on the ADS-B data, we can provide a better source of measurement for air turn performance in addition to the Mode S track and turn reports.

B. Least-square regressions

To find the turn radius, the least-squares regression of a circle is applied to the 2D projections of the 3D positions on a *best* plane. This plane is also found using the least-squares

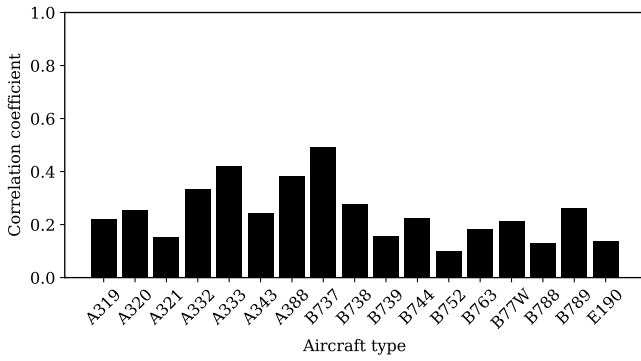


Figure 14. Correlation between speeds and bank angles

method in the first place, with which the distance from all positions is minimized.

In [12], the drawbacks of fitting a 2D circle to 3D points are shown. In this paper, we first transform the 3D point to a 2D plane. Using such a two-step regression is intentional. Firstly, introducing such a plane allows us to reduce the variations in position, as well as to consider the turns with changing of altitude. Secondly, by reducing the dimension of the circle from 3D to 2D, the uncertainty of the estimation is decreased. This leads to a more accurate arc representing the turning trajectory.

C. Turn under heavy wind conditions

During the turn, aircraft commonly maintain a constant airspeed. Thus, wind can have a strong influence on the trajectory of an aircraft during a turn. This influence can be observed from the ground tracks as well. Strong wind can produce a non-circular ground track. The non-symmetric ground track will produce incorrect estimations when the proposed method is applied.

In this paper, we made use of regression errors in Equation 27 to filter out these scenarios where strong wind is present. To further extend the method in the future to take into consideration of wind, we must reconstruct the problem in the form of ordinary differential equations, and then solve the equations using the combination of ADS-B data and wind information from additional sources. It is interesting to point out that some previous studies have also used data from turns to estimate wind [13]–[16].

Knowing the wind information in addition to the ADS-B data would improve the calculation. It is worth noting that flight management systems from different manufacturers may perform the same turn procedures differently. For example, in [17], radius-to-fix experiments were carried out to test these flight management systems. Results showed differences in these test flights, with the most noticeable ones being how the wind, as well as the climb gradient, were handled during the turns.

D. Aircraft mass and turn performance

Aircraft mass has been an important parameter for several aircraft performance-related studies [4], [18]. When an aircraft is turning at low speed, the bank angle needs to be smaller than the maximum allowed bank angle. This limitation leaves a safety margin ensuring that an aircraft does not enter stall conditions. With more accurate information on the bank angle from ADS-B data, additional information on mass can be obtained to improve these aforementioned studies.

The maximum physical limitation of the bank angle is constrained by the maximum lift available and the weight of the aircraft. Knowing an aircraft's aerodynamic characteristics and airspeed, the mass boundary can be calculated. Since the load factor of the aircraft can be computed based on the estimated bank angle, the maximum mass of the aircraft during the turn is:

$$\tilde{m}_{max} = \frac{W_{max}}{g} = \frac{L_{max}}{ng} = \frac{C_{L,max}}{ng} \frac{1}{2} \rho V^2 S \quad (31)$$

where $C_{L,max}$ is the maximum lift coefficient and S is the wing area. Based on this new information, as well as the maximum takeoff weight (m_{mtow}) and the operational empty weight (m_{oew}) of an aircraft, we can reduce the mass interval to:

$$\left[m_{oew}, \min(m_{mtow}, \tilde{m}_{max}) \right] \quad (32)$$

Using the same dataset from the experiment section, we can compute the maximum possible weight of the aircraft at each turn. In Figure 15, the distributions of the possible maximum mass are illustrated as the percentage of the maximum takeoff mass. Note that only turns with maximum masses lower than maximum takeoff masses are included. The number of trajectories compared to all trajectories are indicated in the lower-left corner of each plot.

In this test, we set the maximum lift coefficient as a fixed value of 1.4 for all aircraft. In reality, the maximum lift coefficient differs according to the aircraft type and aerodynamic configurations. Figure 15 demonstrates the additional information on weight obtained by observing the turn.

VII. CONCLUSION

In this paper, we addressed the challenge of estimating aircraft performance parameters during the turning segments of flights based only on ADS-B information during the offline data analysis phase. It provided ways to identify turns in ADS-B trajectories, as well as methods to calculate hidden parameters. In summary, this paper provided new insights on aircraft turn performance for ADS-B data-based studies.

At first, we developed a simple data mining algorithm that made it easy to identify the turn segments in the flight. Once an individual turn was extracted from the flight, we transformed the three-dimensional turning trajectory onto a two-dimensional plane, where the radius of the turn could be computed using least-squares regression.

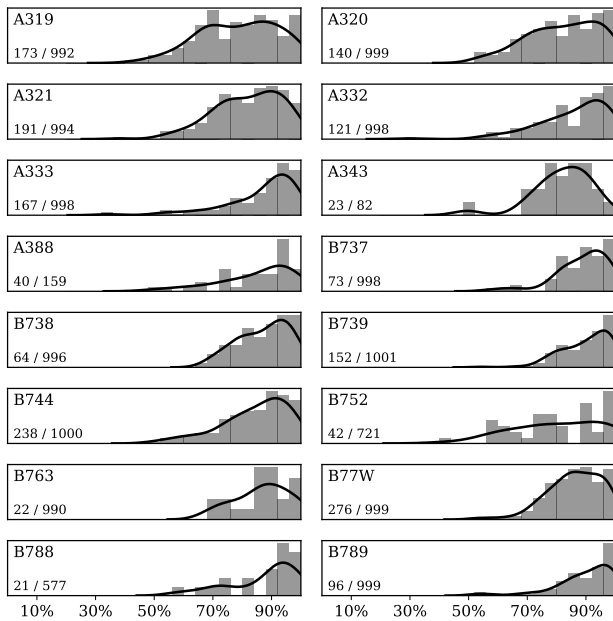


Figure 15. Distribution of maximum flight mass per aircraft type (only $m < m_{mtow}$ are considered, $C_{L,max} = 1.4$)

In this study, we only considered the coordinated turns under light wind conditions. The coordinated turn was a safe assumption for most airliners. However, when heavy wind condition occurs, our method may produce an estimate with errors. We use the least-squares regression error to evaluate whether the wind is an influencing factor during the estimation. In future studies, a more advanced nonlinear estimation method could be investigated to obtain the turn parameters and wind at the same time.

Combining the turn radius and the speed of the aircraft, we were able to compute the bank angle and load factor, as well as the turn rate of the aircraft during the turn. Using the data from secondary Mode-S communications (track and turn report), we were able to validate the estimations derived from ADS-B data. The median errors for bank angle and turn rate were found to be around 2 degrees and 0.05 degree/s respectively.

Knowing parameters such as bank angle and turn rate would bring more accurate information for performance-related research. For instance, we demonstrated that knowing the actual load factor, we were able to increase our knowledge of the aircraft mass. This, in turn, would help to improve other performance parameter estimations in future studies. Furthermore, accurate estimations of turns can also improve the prediction of flight course changes in flight operations. Future studies could also be conducted based on these improved parameters to provide improved trajectory reconstructions and predictions.

REFERENCES

- [1] M. Schäfer, M. Strohmeier, V. Lenders, I. Martinovic, and M. Wilhelm, "Bringing up OpenSky: A large-scale ADS-B sensor network for research," in *Proceedings of the 13th international symposium*

on Information processing in sensor networks, IEEE Press, 2014, pp. 83–94.

- [2] J. Sun, J. Ellerbroek, and J. Hoekstra, "Flight Extraction and Phase Identification for Large Automatic Dependent Surveillance–Broadcast Datasets," *Journal of Aerospace Information Systems*, vol. 14, no. 10, pp. 566–571, 2017. DOI: 10.2514/1.1010520.
- [3] X. Olive, "Traffic, a toolbox for processing and analysing air traffic data," *Journal of Open Source Software*, vol. 4, p. 1518, 2019, ISSN: 2475-9066. DOI: 10.21105/joss.01518.
- [4] J. Sun, H. A. Blom, J. Ellerbroek, and J. M. Hoekstra, "Particle filter for aircraft mass estimation and uncertainty modeling," *Transportation Research Part C: Emerging Technologies*, vol. 105, pp. 145–162, 2019.
- [5] R. Madácsi and R. Markovits-Somogyi, "Bank angle estimation using radar data," *Periodica Polytechnica Transportation Engineering*, vol. 47, no. 1, pp. 1–5, 2019.
- [6] J. Sun, *Open Aircraft Performance Modeling: Based on an Analysis of Aircraft Surveillance Data*. Delft University of Technology, 2019, ch. 8.
- [7] J. D. Anderson, *Aircraft performance and design*. McGraw-Hill Science/Engineering/Math, 1999.
- [8] M. Ester, H. P. Kriegel, J. Sander, and X. Xu, "A Density-Based Algorithm for Discovering Clusters in Large Spatial Databases with Noise," *Second International Conference on Knowledge Discovery and Data Mining*, pp. 226–231, 1996.
- [9] D. Umbach and K. N. Jones, "A few methods for fitting circles to data," *IEEE Transactions on instrumentation and measurement*, vol. 52, no. 6, pp. 1881–1885, 2003.
- [10] A. Al-Sharadqah, N. Chernov, et al., "Error analysis for circle fitting algorithms," *Electronic Journal of Statistics*, vol. 3, pp. 886–911, 2009.
- [11] J. Sun, H. Vũ, J. Ellerbroek, and J. Hoekstra, "PyModeS: Decoding Mode-S Surveillance Data for Open Air Transportation Research," *IEEE Transactions on Intelligent Transportation Systems*, 2019. DOI: 10.1109/TITS.2019.2914770.
- [12] L. Dorst, "Total least squares fitting of k-spheres in n-d euclidean space using an (n+ 2)-d isometric representation," *Journal of mathematical imaging and vision*, vol. 50, no. 3, pp. 214–234, 2014.
- [13] D. Delahaye, S. Puechmorel, and P. Vacher, "Windfield estimation by radar track Kalman filtering and vector spline extrapolation," in *Digital Avionics Systems Conference 2003*, IEEE, vol. 1, 2003. DOI: 10.1109/DASC.2003.1245869.
- [14] D. Delahaye and S. Puechmorel, "TAS and wind estimation from radar data," in *AIAA/IEEE Digital Avionics Systems Conference - Proceedings*, IEEE, 2009, 2–B. DOI: 10.1109/DASC.2009.5347547.
- [15] P. M. A. de Jong, J. J. van der Laan, A. C. i. ' Veld, M. M. van Paassen, and M. Mulder, "Wind-Profile Estimation Using Airborne Sensors," *Journal of Aircraft*, vol. 51, no. 6, pp. 1852–1863, 2014. DOI: 10.2514/1.C032550.
- [16] A. M. P. de Leege, M. M. Van Paassen, and M. Mulder, "Using automatic dependent surveillance-broadcast for meteorological monitoring," *Journal of Aircraft*, vol. 50, no. 1, pp. 249–261, 2012.
- [17] A. A. Herndon, M. Cramer, and K. Sprong, "Analysis of advanced flight management systems (fms), flight management computer (fmc) field observations trials, radius-to-fix path terminators," in *2008 IEEE/AIAA 27th Digital Avionics Systems Conference*, IEEE, 2008, 2–A.
- [18] J. Sun, J. Ellerbroek, and J. Hoekstra, "Aircraft initial mass estimation using Bayesian inference method," *Transportation Research Part C: Emerging Technologies*, vol. 90, pp. 59–73, 2018. DOI: 10.1016/j.trc.2018.02.022.